Parity and signature test for the vector-vector system (revisited)

Mikhail Mikhasenko[1,*]

[1] CERN-EP, CH-1211, Geneva, Switzerland

(Dated: June 18, 2020)

We present a construction of the reaction amplitude for inclusive production of the resonance decaying to a pair of identical vectors, as $J/\psi J/\psi$, $\phi\phi$, Z^0Z^0. The method provides possibility to determine the spin and parity of the resonance in the model-independent way. The test of the quantum-number hypotheses is demonstrated on the Standard Model decay of the Higgs particle to four leptons.

I. INTRODUCTION

Formation of the hadronic matter is one of a few ununderstood parts of Quantum Chromodynamics (QCD) leaving a little black spot in the Standard Model. Despite the fact that QCD is the fundamental theory of strong interaction, the theory degrees of freedom change at the low energy where hadronic phenomena emerges. Whilst the constituent quark model successfully describes the majority of the observed hadronic states, not all. Over the last decade we have witnessed overwhelming evidence of unexpected phenomena beyond the quark model that includes the observation of XYZ states in the charminium spectrum [1], the pentaquark states [2, 3], as well as the resonance-like phenomena of the hadron rescattering singularizes [4]. The spin-parity of the observed exotica is a critical part of the formation puzzle, and moreover, in most of the cases it can be determined experimentally. Nevertheless, the separation of the spin hypothesis is often rather cumbersome and requires case-by-case treatment. In the paper we revisit the problem of the spin-parity assignment for the system two identical vectors with their possible further decay.

We anticipate three applications of the presented framework. First, the fresh observation of the threshold enhancement in the $J/\psi J/\psi$ spectrum [5] that might lead to a new milestone in the understanding of the hadron formation through the mechanism for binding four charm quarks [6]. Second, the $\phi\phi$ pairs produced in central exclusive reactions hint a resonance signal, that is a candidate for a tensor glueball [7, 8]. The proposed approach sets the ground for the complete partial wave analysis of the high statistics $pp \to pp\,K^+K^-K^+K^-$ that should be possible with the modern LHC data. Thirdly, one find the same vector-vector signature in the Standard Model (SM) decay of the Higgs boson, $H \to Z^0Z^0$. To conclude in favor of 0^+ hypothesis for the spin-parity of the Higgs boson several phenomenological models were compared on the combined dataset of several decay channels [9, 10]. In contrast, we discuss the anatomy of the assumption-free approach.

The two key constraints that determine the properties of the decay are the parity conservation and the permutation symmetry. One consequence of these constraints is known as the Landau-Yang theorem [11, 12]. The theorem states that a massive boson with $J^P = 1^\pm$ cannot decay into two on-shell photons. The statement follows naturally from the general equations we provide. Moreover, the extension of the selection rule to all the natural quantum numbers with odd spin is easily obtained. A parity-signature test of a signal in $\phi\phi$ system have been discussed in the past by several authors [13, 13, 13–15]. We derive the results consistent with the previous works using the modern conventions on the state vectors and rotation matrices. Also, we suggest exploring the spin-parity hypothesis using the full power of the multidimensional test statistics.

The paper is organized as follows. The reaction amplitude is presented in Sec. II. In Sec. III we discuss the symmetry constraints. We describe the test-statistics discriminator in Sec. IV. The method is demonstrated on the SM Higgs decay in Sec. V.

II. ANGULAR AMPLITUDE

We focus on an inclusive production process $pp' \to X + \ldots$, where X is a resonance decaying to two vector mesons. Despite the vectors are identical, it is convenient to distinguish them in the reaction amplitude calling them V_1 and V_2. In that way, we can make sure that the amplitude is symmetric on the permutation of indices 1 and 2.

[*] e-mail: mikhail.mikhasenko@cern.ch

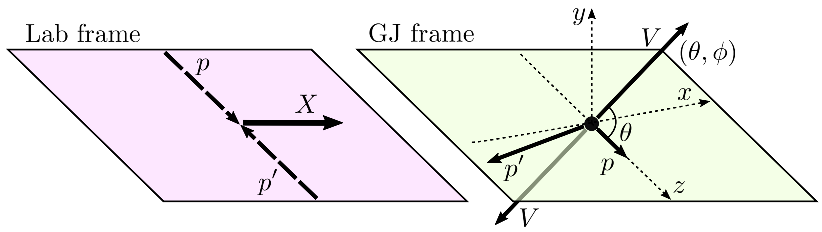

FIG. 1: Schematic view of production kinematics of X state at the pp collider. The Gottfried-Jackson frame is used for describing production kinematics. It is defined in the rest frame of X by the vectors of the beam particles: $\vec{z} = \vec{p}/|\vec{p}|$, $\vec{y} = \vec{p}' \times \vec{p}/|\vec{p}' \times \vec{p}|$, $\vec{x} = \vec{y} \times \vec{z}$. The spherical angles (θ, ϕ) are the angles of one of two decay vectors in the GJ frame. The black arrows shows three dimensional vectors of particles. The three-momenta of the produced vectors are $\vec{p}_{V_1}$ and $\vec{p}_{V_2}$.

The production frame is set up in the rest frame of X as a plane that contains three-vectors of the production reaction, i.e. $\vec{p}$, and $\vec{p}'$. The normal to the plane gives y axis (precisely $\vec{p}' \times \vec{p}$) as shown in Fig. 1. We use the Gottfried-Jackson (GJ) frame for defining in the x and z axis in the production plane [16]. We note that the choice of x and z axes is not unique, two other two common definition of the production frame are the helicity (HX) frame defined by the direction of motion of X itself in the lab frame, and the Collins-Soper (CS) frame where z is defined by bisection of the angle between $\vec{p}$ and $\vec{p}'$ [17].

We consider a general case of arbitrary polarization of X. We note that a negligibly small polarization is measured in the prompt production of charmonium ("head on" collisions) [18–22]. In opposite, for the peripheral processes, e.g. central exclusive production (CEP) a significant polarization is expected [23].

The full kinematics of the decay is described by 6 angles: a pair of sperical angles (θ, ϕ) of the momentum of V_1 in the GJ frame, and two pairs of the spherical angles (θ_i, ϕ_i), $i = 1, 2$ for the decays of the vector mesons in their own helicity frames. We note that the angles ϕ_i can also be defined in the X rest frame as shown in Fig. 2 since they are not effected by the boosts along the vector-meson directions of momentum.

The spin of the decay particle X defines rotational properties of the system of the decay products [24]. Every configuration of the three-momenta of the final-state particles in the X rest frame can be considered as a solid body for which the orientation is described by three angles: the pair of the spherical angles (θ, ϕ) describe the direction of $\vec{p}_{V_1}$, the third angle ϕ_1 is the azimuthal direction of μ^+ (see Fig. 1 and Fig. 2). For the sake of certainty, we consider the decay $X \to V(\mu^+\mu^-)V(\mu^+\mu^-)$ in the main text. A mild modification one needs to implement for $X \to V(K^+K^-)V(K^+K^-)$ are given in Appendix A. The normalized differential cross section denoted by the intensity I reads:

$$I(\Omega, \Omega_1, \Omega_2) = (2J+1) \sum_{M,M'} R_{M,M'}\, D^J_{M,\nu}(\phi, \theta, \phi_1) D^{J*}_{M',\nu'}(\phi, \theta, \phi_1) \sum_{\xi_1,\xi_2}^{\{-1,1\}} A^{\nu}_{\xi_1,\xi_2}(\Omega_1, \Omega_2) A^{\nu'*}_{\xi_1,\xi_2}(\Omega_1, \Omega_2), \tag{1}$$

where we have explicitly separated the production and decay part of the amplitude. The production dynamics is encapsulated into the polarization matrix $R_{M,M'}$. The decay amplitude is denoted by $A^{\nu}_{\xi_1,\xi_2}$ with ν being the difference of the vector-meson's helicities, and ξ being the difference of the muon's helicities. J and M are the spin and the spin projection of the X. The decay amplitude is described by the remaining three angles: θ_1, θ_2, and $\Delta\phi = \phi_2 - \phi_1$ (see Fig. 2).

$$A^{\nu}_{\xi_1,\xi_2}(\theta_1, \theta_2, \Delta\phi) = 3 \sum_{\lambda_1,\lambda_2} \delta_{\nu,\lambda_1-\lambda_2} (-1)^{1-\lambda_2} H_{\lambda_1\lambda_2} d^1_{\lambda_1,\xi_1}(\theta_1) d^1_{\lambda_2,\xi_2}(\theta_2) e^{i\lambda_2\Delta\phi} \tag{2}$$

The factor $(-1)^{1-\lambda_2}$ is related to the Jacob-Wick particle-2 phase convention [25]. Once the phase is factored out of the helicity coupling matrix H_{λ_1,λ_2}, the symmetry relations for H are significantly simpler as presented in the next section.

III. SYMMETRY CONSTRAINTS

The matrix of the helicity couplings is strictly defined by

$$H_{\lambda_1,\lambda_2} = \langle JM; \lambda_1, \lambda_2 | \hat{T} | JM \rangle\,, \tag{3}$$

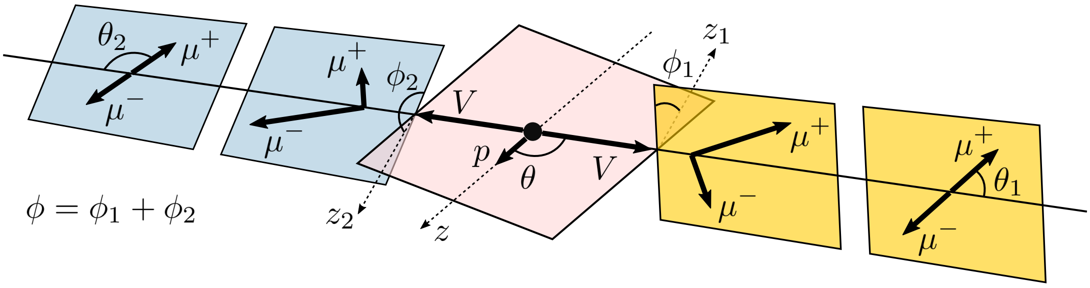

FIG. 2: Schematic view of the $X \to V(\mu^+\mu^-)\,V(\mu^+\mu^-)$ decay kinematics. The central three planes show orientation of vectors in the X rest frame. The right and left most planes show the decay angles of J/ψ_1 and J/ψ_2 in the rest frame, respectively.

TABLE I: Possible quantum numbers of the decaying particle X separated to four groups with respect of symmetry of the helicity matrix. The framed quantum numbers in the last column have additional restrictions due to the maximal value of the spin projection.

group	parity of J, $(-1)^J$	naturality, $P(-1)^J$	explicit J^P
I	even(+)	natural(+)	$\boxed{0^+}$, 2^+, 4^+, 6^+
II	even(+)	unnatural(−)	$\boxed{0^-}$, 2^-, 4^-, 6^-
III	odd(−)	natural(+)	1^-, 3^-, 5^-, 7^-
IV	odd(−)	unnatural(−)	$\boxed{1^+}$, 3^+, 5^+, 7^+

where the bra-state is the protected two-particle state in the particle-2 convention, the ket-state is the decaying state with the defined spin J and the spin projection to the z axis in the GJ frame, M [26, 27]. The elements of the helicity matrix are, in general, arbitrary complex numbers. However, the matrix is constrained by parity and permutation symmetry. The parity transformation relates the opposite values of the vectors' helicities:

$$H_{\lambda_1,\lambda_2} = P(-1)^J H_{-\lambda_1,-\lambda_2}, \tag{4}$$

with P being the internal parity of X. The identity of the vector mesons relates the helicity matrix with the transposed one:

$$H_{\lambda_1,\lambda_2} = (-1)^J H_{\lambda_2,\lambda_1}, \tag{5}$$

The matrices of the helicity couplings are symmetric (anti-symmetric) for the even (odd) spin (spin) J. Combining the two symmetries we split all possible quantum numbers J^P into four groups as shown in Tab. I. The relations Eq. (4) and Eq. (5) greatly reduce the number of free components of the helicity matrix.

$$H_I = \begin{pmatrix} b & a & c \\ a & d & a \\ c & a & b \end{pmatrix}_S \qquad H_{II} = \begin{pmatrix} b & a & \\ a & & -a \\ & -a & -b \end{pmatrix}_S \qquad H_{III} = \begin{pmatrix} & a & \\ -a & & -a \\ & a & \end{pmatrix}_A \qquad H_{IV} = \begin{pmatrix} & a & c \\ -a & & a \\ -c & -a & \end{pmatrix}_A \tag{6}$$

There are three special cases, 0^+ of the first group for which $a = c = 0$, 0^- in the second group with $a = 0$, and 1^+ in the forth group with $c = 0$. One finds that the helicity matrices are orthogonal to each other, with the scaler product defined by $(H_1 \cdot H_2) = \mathrm{Tr}(H_1 H_2^\dagger)$. The four groups produce generally different angular distribution except a few generate cases discussed in Appendix C.

The form of the helicity matrices in Eq. (6) immediately leads to the conclusion of the Landau-Yang theorem [11, 12]. For the decay of X to a pair of the real photons, $H_{0,\lambda} = H_{\lambda,0} = 0$, as the photon cannot carry the longitudinal polarization, $\lambda = 0$. Practically, one must cross the second row and the second column of the helicity matrix. The matrix of the group-*III* completely vanishes, there are no helicity couplings that the decay can process with. Hence, the mesons with the odd-natural J^P quantum number cannot decay to two real photons. The special case of group-*IV* with $c = 0$ vanishes as well making the decay of $J^P = 1^+$ to two real photons forbidden.

IV. TESTING HYPOTHESIS

The most powerful method for testing spin hypothesis is the multidimensional fit. For simplicity we consider the case of the negligible polarization in three dimensions, while all discussion is easy to generalize to the five dimensional case that includes the polarization degrees of freedom. The test statistics is defined by

$$\mathrm{TS}_{M/M'} = \mathrm{LLH}_M - \mathrm{LLH}_{M'}, \tag{7}$$

, where the LLH_M is the maximized value of the log likelihood over the set of helicity couplings.

$$\mathrm{LLH}_M = \frac{1}{N_{\mathrm{ev}}} \sum_{e=1}^{N_{\mathrm{ev}}} \log I(\tau_e | M\{\hat{h}\}). \tag{8}$$

The intensity $I(\tau_e|\hat{c})$ is calculated for the kinematic variables of the event e. The optimized model parameters are demoted by $\hat{h}$. We use a convenient normalization condition $\mathrm{Tr}(HH^\dagger) = 1$.

Distribution over $\Delta\phi$ angle once θ_1 are θ_2 are integrated:

$$\frac{2\pi}{N}\frac{\mathrm{d}N}{\mathrm{d}\Delta\phi} = 1 + \frac{h_{1,1}h^*_{-1,-1}}{2}\cos(2\Delta\phi), \tag{9}$$

The sign of the $\cos(2\Delta\phi)$ component depends on J^P: it is positive for quantum numbers of the first group, and negative for the ones in the second group. The decays from the third and fourth groups wound not show any $2\Delta\phi$ dependence.

V. TESTING THE STANDARD MODEL HIGGS DECAY

To demonstrate the method The most famous particle decaying to two identical vectors is the Higgs boson. In order to validate out approach we performed analysis of the reaction $H \to Z(\mu^+\mu^-)Z(\mu^+\mu^-)$. The interaction vertex of Higgs with a pair of Z^0 bosons is $2im_Z^2/v\, g^{\mu\nu}$, hence the helicity amplitude reads:

$$A^{H\to ZZ}_{\lambda_1,\lambda_2} = 2i\frac{m_Z^2}{v}(\varepsilon_1^*(\lambda_1)\cdot\varepsilon_2^*(\lambda_2)). \tag{10}$$

Using the explicit expressions for the polarization ε vectors (see Appendix B), we find a special case of the matrix for group-I,

$$H^{H\to ZZ} = \frac{\mathbb{I}}{\sqrt{3}} + O(p^2) \tag{11}$$

The matrix is proportional to identity (S-wave) close to the nominal Z^0Z^0 production threshold, the contribution of the D-wave is suppressed by $|\vec{p}|^2/m_Z^2$.

To test the method presented in Sec. IV a sample of synthetic events is generated and fitted by the different hypotheses using a dedicated framework written in `Julia` [28]. We find that the hypotheses are sufficiently separated already with 500 events. A poll of 500 samples corresponding to the helicity matrix in Eq. (11) is fit by all group hypotheses adjusting the couplings a, b, c, d in order to maximize event-based likelihood in Eq. (8). This maximal values are histogrammed over the poll and are shown in the right panel of Fig. 3. One sees that the group-I hypothesis over-performs others in average despite the statistics fluctuations. The separation is even larger once the test statistics from Eq. (7) is computed for every sample in the poll. The right panel of Fig. 3 shows the comparison of the group-I and the selected alterative hypotheses, the group-III. The distribution of $\mathrm{TS}_{0^+/1^-}$ over the poll is entirely above zero. The test statistics on the 1^- generated data is calculated by creating the second poll corresponding to the matrix H_{III} with $a = 1/\sqrt{3}$. As expected, the 1^- hypothesis is found to have the highest likelihood in average over the second poll. The green distribution in right panel of Fig. 3 is largerly negative. As stressed above, an important part of the separation power comes from the $\Delta\phi$ distribution. Fig. 4 an example of $\mathrm{d}N/\mathrm{d}\phi$ for the two combined sample of the first poll.

VI. CONCLUSION

We have derived an amplitude for the hadronic production of two identical vector-meson system in a model-independent framework. As resonances lead to the structured angular distributions due to well-definite J^P quantum numbers, we show that four groups of J^P separated by the parity of J and the naturality of J^P can be distinguish based on angular distributions. The test-statistics discriminator is proposed. The power of the three-dimensional analysis is demonstrated using the Standard Model Higgs decay to a pair of the Z bosons.

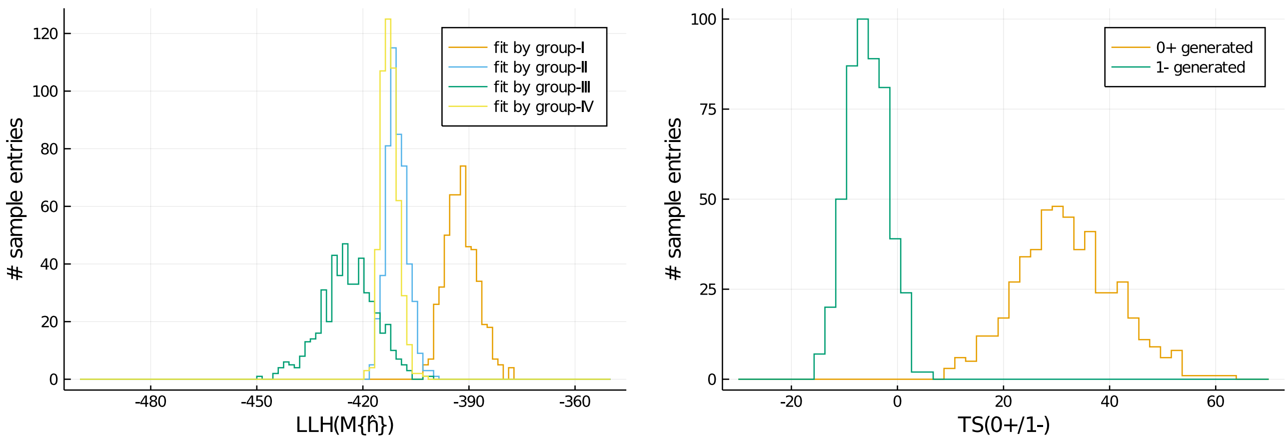

FIG. 3: Test statistics distribution testing hypothesis of groups $I - IV$ and the special cases on the statistical ensemble of the 500 events data samples generated based on the fixed group-III coupling matrix.

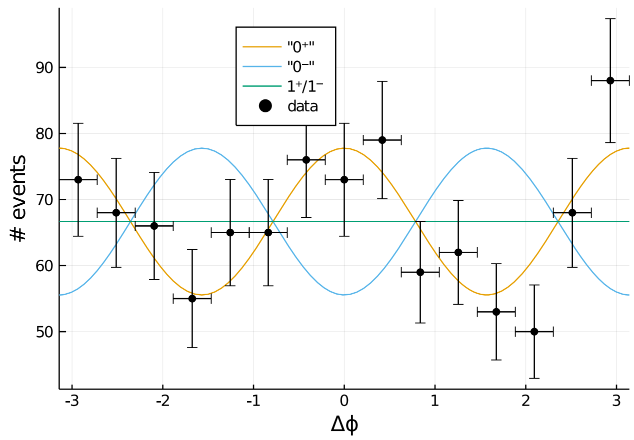

FIG. 4: Distribution of the polar angle $\Delta\phi$ for the Higgs decay to $\mu^+\mu^-\mu^+\mu^-$ with 1000 synthetic events. The orange line is the expectation curve under the $J^P = 0^+$ hypotheses with $b = d = 1/\sqrt{3}$. The distribution is expected to be flat if J is odd. The blue line gives an example of the even-unnatural J^P quantum numbers (group-II).

Acknowledgement

The project was motivated by a discussion in the LHCb Amplitude Analysis group. We thank Biplab Day for organizing seminar dedicated to $X \to VV$. We would like to gratefully thank Alessandro Pilloni for useful comments on the work. We thank Liupan An and Ronan McNulty for finding practical cases for the analysis.

APPENDIX A: MODIFICATIONS FOR $X \to V(K^+K^-)V(K^+K^-)$

The only place that requires modification when the $\phi\phi$ system is considered is the decay matrix element in Eq. (2):

$$A^\nu(\theta_1, \theta_2, \Delta\phi) = 3 \sum_{\lambda_1, \lambda_2} \delta_{\nu, \lambda_1 - \lambda_2} (-1)^{1-\lambda_2} H_{\lambda_1 \lambda_2} d^1_{\lambda_1, 0}(\theta_1) d^1_{\lambda_2, 0}(\theta_2) e^{i\lambda_2 \Delta\phi} \tag{A1}$$

where the decay $\phi \to K^+K^-$ proceeds in P-wave only.

APPENDIX B: POLARIZATION VECTORS

To translate a covatiant expression in Eq. (10) to helicity amplitude the explicit expressions for the polarization vectors are used:

$$\varepsilon_z^\mu(\pm 1) = \frac{1}{\sqrt{2}}\,(0, \mp 1, -i, 0)\,, \qquad \varepsilon_z^\mu(0) = \frac{1}{m_Z}\,(p, 0, 0, E)\,, \tag{B1}$$

where E, p, and m_Z are the energy, momentum, and the mass of the Z boson. The general expressions for the rotational vectors follows:

$$\varepsilon_1(\lambda) = R_z(\phi)R_y(\theta)\varepsilon_z(\lambda), \tag{B2}$$

$$\varepsilon_2(\lambda) = (-1)^{1-\lambda}R_z(\phi)R_y(\theta)R_y(\pi)\varepsilon_z(\lambda), \tag{B3}$$

$$\tag{B4}$$

where $R_y(\phi)R_y(\theta)$ is a product of the three-dimensional rotation matrices that transforms the vector $(0, 0, 1)$ to the direction $(\sin\theta\cos\phi,\, \sin\theta\sin\phi,\, \cos\theta)$. The particle-2 requires additional rotation by π about the y axis. We also use the particle-two phase convention, $(-1)^{1-\lambda_2}$ that adds an extra sign to the vector $\varepsilon_2(0)$.

APPENDIX C: THE Ps INVARIANCE

The helicity coupling matrices from different groups in Eq. (6) do not overlap, moreover, they are all orthogonal to each other. Nevertheless, there are potential cases where different hypothesis are not distinguishable. An example that demonstrate such degeneracy is the following:

$$H^{(\mathrm{deg.})} = \begin{pmatrix} 0 & 1 & 0 \\ s & 0 & sP \\ 0 & P & 0 \end{pmatrix}, \tag{C1}$$

where s is the parity of J, and P is the naturality of J^P. The matrix of this type is present in all groups for different values of s and P The intensity of the unpolarized decay can be computed explicitly [29]:

$$\begin{aligned} I(H) = {}& \frac{s^2P^2\sin^2(\theta_1)\cos^2(\theta_2)}{2} + \frac{s^2P^2\sin^2(\theta_1)}{2} + \frac{s^2\sin^2(\theta_1)\cos^2(\theta_2)}{2} + \frac{s^2\sin^2(\theta_1)}{2} \\ & + \frac{sP\left(\cos(-2\theta_1 + 2\theta_2 + \Delta\phi) + \cos(2\theta_1 - 2\theta_2 + \Delta\phi) - \cos(2\theta_1 + 2\theta_2 - \Delta\phi) - \cos(2\theta_1 + 2\theta_2 + \Delta\phi)\right)}{8} \\ & + \frac{P^2\sin^2(\theta_2)\cos^2(\theta_1)}{2} + \frac{P^2\sin^2(\theta_2)}{2} + \frac{\sin^2(\theta_2)\cos^2(\theta_1)}{2} + \frac{\sin^2(\theta_2)}{2} \end{aligned} \tag{C2}$$

The expression does not change under the flip of P and s sign simultaneously. Hence, the group-*II* with $b = 0$ is undistinguished from the group-*III*, and the group-*I* with $b = d = c = 0$ have the same angular distributions as the group-*IV* with $c = 0$. Such vanishing of the helicity couplings, however, must be an exceptional case indicating some peculiar physical reason.

---

[1] S. Godfrey and S. L. Olsen, Ann. Rev. Nucl. Part. Sci. **58**, 51 (2008), 0801.3867.
[2] R. Aaij et al. (LHCb), Phys. Rev. Lett. **115**, 072001 (2015), 1507.03414.
[3] R. Aaij et al. (LHCb), Phys. Rev. Lett. **122**, 222001 (2019), 1904.03947.
[4] M. Alexeev et al. (2020), 2006.05342.
[5] R. Aaij et al. (LHCb), Phys. Rev. Lett. **XXX**, 222001 (2020), XXXX.XXXXX.
[6] Y.-R. Liu, H.-X. Chen, W. Chen, X. Liu, and S.-L. Zhu, Prog. Part. Nucl. Phys. **107**, 237 (2019), 1903.11976.
[7] D. Barberis et al. (WA102), Phys. Lett. B **474**, 423 (2000), hep-ex/0001017.
[8] P. Lebiedowicz, O. Nachtmann, and A. Szczurek, Phys. Rev. D **99**, 094034 (2019), 1901.11490.
[9] G. Aad et al. (ATLAS), Phys. Lett. B **726**, 120 (2013), 1307.1432.
[10] (2018).
[11] C.-N. Yang, Phys. Rev. **77**, 242 (1950).

[12] L. Landau, Dokl. Akad. Nauk SSSR **60**, 207 (1948).
[13] T. Trueman, Phys. Rev. D **18**, 3423 (1978).
[14] N.-P. Chang and C. Nelson, Phys. Rev. Lett. **40**, 1617 (1978).
[15] J. C. Collins and D. E. Soper, Phys. Rev. D **16**, 2219 (1977).
[16] K. Gottfried and J. D. Jackson, Nuovo Cim. **33**, 309 (1964).
[17] P. Faccioli, C. Lourenco, J. Seixas, and H. K. Wohri, Eur. Phys. J. C **69**, 657 (2010), 1006.2738.
[18] R. Aaij et al. (LHCb), Eur. Phys. J. C **73**, 2631 (2013), 1307.6379.
[19] S. Chatrchyan et al. (CMS), Phys. Rev. Lett. **110**, 081802 (2013), 1209.2922.
[20] T. Aaltonen et al. (CDF), Phys. Rev. Lett. **108**, 151802 (2012), 1112.1591.
[21] R. Aaij et al. (LHCb), Phys. Lett. B **724**, 27 (2013), 1302.5578.
[22] A. M. Sirunyan et al. (CMS), Phys. Rev. D **97**, 072010 (2018), 1802.04867.
[23] R. Pasechnik, A. Szczurek, and O. Teryaev, Phys. Rev. D **83**, 074017 (2011), 1008.4325.
[24] M. Mikhasenko et al. (JPAC), Phys. Rev. D **101**, 034033 (2020), 1910.04566.
[25] M. Jacob and G. Wick, Annals Phys. **7**, 404 (1959).
[26] A. D. Martin and T. D. Spearman, *Elementary-particle theory* (North-Holland, Amsterdam, 1970), URL `https://cds.cern.ch/record/102663`.
[27] P. D. B. Collins, *An Introduction to Regge Theory and High-Energy Physics*, Cambridge Monographs on Mathematical Physics (Cambridge Univ. Press, Cambridge, UK, 2009), ISBN 9780521110358, URL `http://www-spires.fnal.gov/spires/find/books/www?cl=QC793.3.R4C695`.
[28] *The `JpsiJpsi` framework implemented in `Julia`*, Available at `https://github.com/mmikhasenko/JpsiJpsi.jl`.
[29] A. Meurer, C. P. Smith, M. Paprocki, O. Čertík, S. B. Kirpichev, M. Rocklin, A. Kumar, S. Ivanov, J. K. Moore, S. Singh, et al., PeerJ Computer Science **3**, e103 (2017), ISSN 2376-5992, URL `https://doi.org/10.7717/peerj-cs.103`.